Semicond. Sci. Technol. **14** (1999) 1154–1160. Printed in the UK PII: S0268-1242(99)03557-9

Formation of misfit dislocations during growth of $In_xGa_{1-x}As$/GaAs strained-layer heterostructures

X W Liu†, A A Hopgood†, B F Usher‡, H Wang§ and N St J Braithwaite†

† The Open University, Faculty of Technology, Walton Hall, Milton Keynes MK7 6AA, UK
‡ La Trobe University, Department of Electronic Engineering, Bundoora, Victoria 3083, Australia
§ Nanyang Technological University, Microelectronics Centre, School of Electrical and Electronic Engineering, Singapore 639798

Received 19 April 1999, in final form 6 August 1999, accepted for publication 16 September 1999

Abstract. Transmission electron microscopy of GaAs/$In_xGa_{1-x}As$/GaAs double heterostructures has enabled the onset and subsequent development of misfit dislocations to be followed for increasing strained-layer thicknesses, from sub- to supercritical. It has been observed that misfit segments are introduced into threading dislocations when the strained-layer thickness is close to, but below, the critical thickness predicted by the Matthews–Blakeslee (M–B) model. Analysis shows that threading dislocations may be able to glide to form interfacial misfit dislocation segments even though the critical thickness predicted by the M–B model has not been reached. It has also been observed that the total dislocation density rises slowly as the layer thickness increases above its critical value, until a sudden increase occurs. It is suggested that the sudden increase in dislocation density is associated with a different mechanism of misfit dislocation formation, which dominates the global relaxation of the structure.

1. Introduction

For lattice-mismatched epitaxial layers, it is widely accepted that there exists a critical thickness beyond which misfit dislocations are introduced causing the breakdown of coherence between the substrate and epitaxial layers. The critical thickness is defined as the thickness at which the first misfit dislocation nucleates. The transformation of threading dislocations, bowing and elongating to form misfit segments under the effect of misfit stress, has been taken as the mechanism which determines the critical thickness [1–3].

In this paper, the transformation of threading dislocations observed by transmission electron microscopy (TEM) in GaAs/$In_xGa_{1-x}As$/GaAs double heterostructures is reported. As TEM allows direct imaging of individual dislocations, it is one of the most sensitive techniques for investigating the formation of misfit dislocations. Furthermore, specimens prepared by the epilayer lift-off (ELO) technique provide a much larger area for investigation than can be achieved by other TEM specimen preparation techniques such as ion beam and chemical etching.

2. The Matthews–Blakeslee model and its limitations

Matthews and coworkers [1–3] proposed a relaxation mechanism for lattice-mismatched epilayers, known as the Matthews–Blakeslee (M–B) model. In this model, threading dislocations elongate to form misfit dislocation segments under the influence of the misfit stress, and the critical thickness can be predicted from the forces acting on the dislocations. The two main forces are F_ε, acting to elongate the threading dislocation in the interface due to the misfit strain, and F_l, the dislocation line tension resisting the elongation of a dislocation.

Three stages of threading dislocation transformation have been predicted, corresponding to different levels of strained-layer thickness in the structure. At stage I (figure 1(*a*)) where $F_\varepsilon < 2F_l$, the threading dislocation remains straight and the interfaces between layers are coherent. At stage II (figure 1(*b*)), where $F_\varepsilon = 2F_l$, the threading dislocation becomes bowed. At stage III (figure 1(*c*)), where $F_\varepsilon > 2F_l$, the dislocation elongates along both interfaces. This elongation reduces the misfit strain and destroys the coherence of the interfaces between layers.

The concept of critical thickness based on this model is established by balancing the forces acting on the dislocation

0268-1242/99/121154+07$30.00

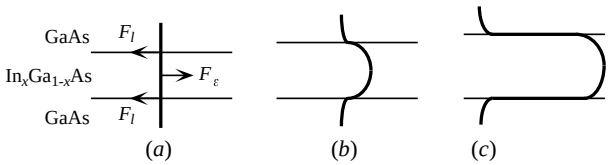

Figure 1. M–B model of misfit dislocation formation. (*a*) Stage I: threading dislocation in coherent interface. (*b*) Stage II: critical point. (*c*) Stage III: incoherent interface.

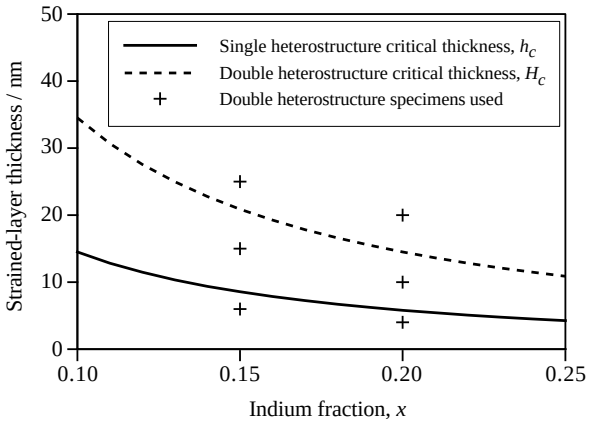

Figure 2. Critical thickness predicted by the M–B model for $In_xGa_{1-x}As/GaAs$ heterostructures.

line. For the structure shown in figure 1, if the layers are isotropic and have the same elastic constants, then

$$F_\varepsilon = \frac{2G(1+\nu)}{(1-\nu)} bh\varepsilon \cos\lambda$$

and

$$F_l = \frac{Gb^2}{4\pi(1-\nu)}(1-\nu\cos^2\alpha)\left(\ln\frac{h}{b}+1\right)$$

where G is the shear modulus of the layers A and B, ν Poisson's ratio, b the Burger's vector, h the strained-layer thickness, ε the misfit strain, α the angle between the dislocation line and its Burger's vector, and λ the angle between the slip direction and the direction in the film plane that is perpendicular to the line of intersection of the slip plane and the interface.

The strained-layer thickness at which $F_\varepsilon = 2F_l$ is defined as the double-heterostructure critical thickness, H_c, and is given by

$$H_c = \frac{b}{4\pi f}\frac{(1-\nu\cos^2\alpha)}{(1+\nu)\cos\lambda}\left(\ln\frac{H_c}{b}+1\right)$$

where f is the lattice mismatch. For a single heterostructure, the critical thickness h_c can be derived by setting $F_\varepsilon = F_l$. Figure 2 gives the critical thickness curves as a function of indium concentration for $In_xGa_{1-x}As/GaAs$ single and double heterostructures based on the M–B model.

The M–B model is the established basis for critical thickness determination, and Pichaud *et al* [4] have recently claimed that the M–B mechanism could actually be observed in low-misfit systems. The model is expected to predict

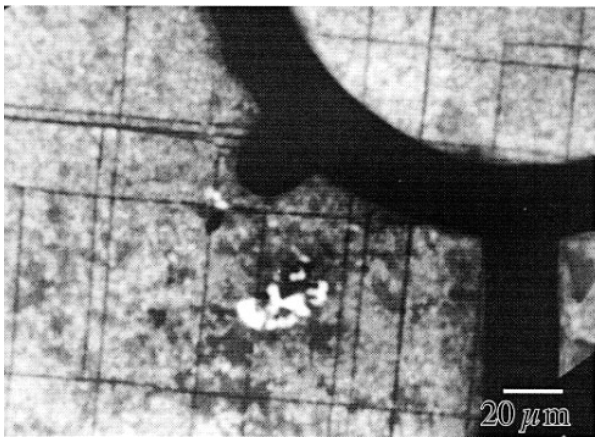

(*a*)

(*b*)

Figure 3. CL images of misfit dislocations in $GaAs/In_{0.15}Ga_{0.85}As/GaAs$ heterostructures: (*a*) after attachment of grid but before ELO; (*b*) after ELO.

accurately the critical thickness for strains of up to approximately 1% [5]. However, as a result of analytic approximations in the M–B theory, the predicted critical thicknesses are double valued at low strains and non-existent at higher strains [6]. Where two values are yielded, the lower value is considered unphysical as it is of the order of one Burger's vector.

Although equilibrium theory predicts when a threading dislocation could be turned over to form a misfit dislocation, what happens next is a matter of chance [7]. Dixon and Goodhew [8] found that, in $In_xGa_{1-x}As$ grown on GaAs by molecular-beam epitaxy (MBE), threading dislocations were turned over at a thickness near the equilibrium critical thickness, but the generation of fresh dislocations did not take place until a much greater thickness. Whitehouse *et al* [9] found different phases of relaxation in $In_xGa_{1-x}As$ grown on GaAs. Threading dislocations played the dominant role in the first phase; after all $(a/2)\langle 110\rangle$ type dislocations had been activated, a significant increase in the epilayer thickness was required to initiate a second phase of stress relief resulting from other dislocation generation processes. Kidd *et al* [10] illustrated the transition from the appearance of the first misfit dislocations in thin layers, which only provided localized relaxation, to the condition where the dislocation density was sufficient to relax all regions of the layer.

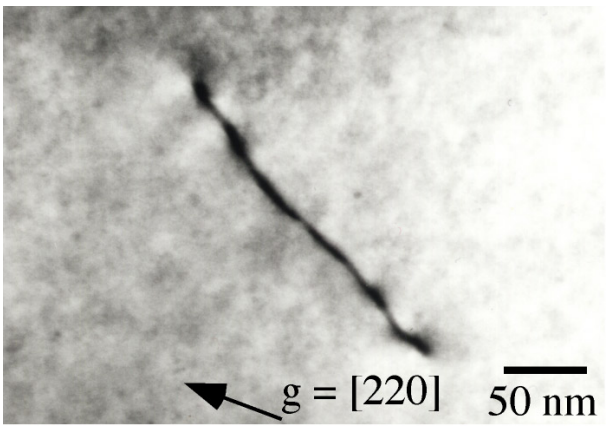

Figure 4. Threading dislocations in GaAs.

3. Experimental method

3.1. GaAs/$In_xGa_{1-x}As$/GaAs growth

All specimens were grown by MBE. A 0.25 μm GaAs buffer layer and a 50 nm AlAs layer were firstly grown on a GaAs (001) substrate, followed by epitaxial heterostructures consisting of an $In_xGa_{1-x}As$ layer of variable thickness between two 200 nm GaAs layers. The growth temperature was 530 °C for the $In_xGa_{1-x}As$ layers and 600 °C for other layers; the growth rate was approximately 1 μm h^{-1}. The molar fractions of indium (i.e. x in $In_xGa_{1-x}As$) were 0, 0.15 and 0.2. The designed thicknesses, h, were 6, 15 and 25 nm for $x = 0.15$ and 4, 10 and 20 nm for $x = 0.2$. The composition and layer thickness were calibrated by x-ray diffraction, and monitored during growth by reflection high-energy electron diffraction. This combination of calibration and monitoring gives consistent accuracy for composition of better than ±5%. The layer thicknesses were subsequently checked by cross-sectional TEM.

3.2. TEM specimen preparation

With the exception of the cross-sectional TEM measurements, the specimens for observation by TEM were prepared by ELO. This technique relies on the presence of an AlAs layer to release the heterostructures from the substrate. The lattice parameters of GaAs (0.5653 nm) and AlAs (0.5661 nm) are sufficiently close [11] that the inclusion of an AlAs layer in the specimens does not introduce significant strain.

The GaAs/$In_xGa_{1-x}As$/GaAs layers, together with a pre-attached copper grid, were floated off by chemically etching the AlAs layer with 10% HF. The grid was glued onto the specimen surface before separating the heterostructure, rather than afterwards, as this was found to make handling easier and to produce higher-quality TEM specimens. Details of the ELO procedure are as follows.

(a) The specimens were cleaved to a square (approximately 3 mm × 3 mm).
(b) The specimen surface was cleaned with acetone.
(c) A 200 or 400 mesh copper grid was stuck to the surface using a cyanoacrylate adhesive.

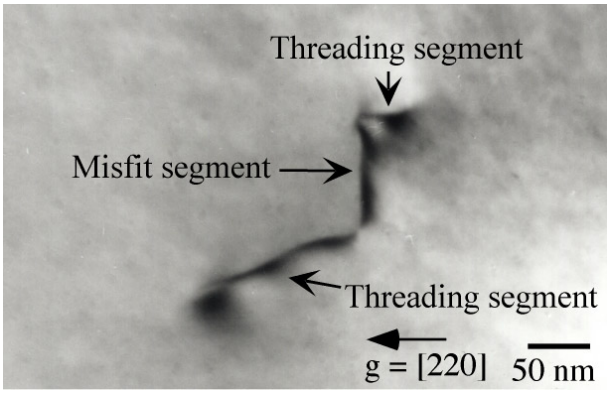

(*a*)

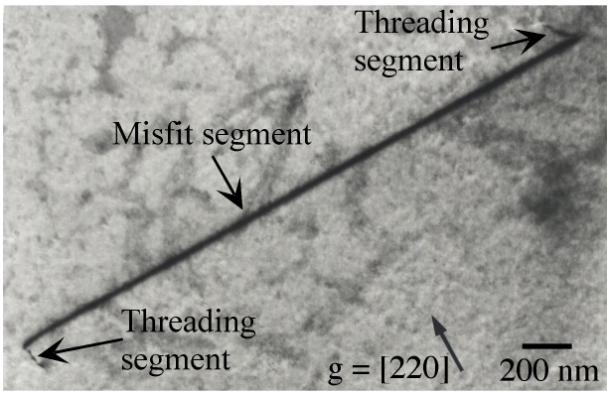

(*b*)

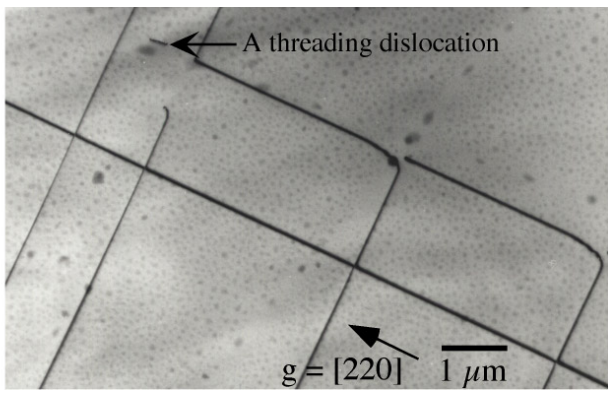

(*c*)

Figure 5. Dislocations in GaAs/$In_{0.15}Ga_{0.85}As$/GaAs: (*a*) misfit dislocation segment, $h = 6$ nm; (*b*) elongated misfit dislocation segment, $h = 15$ nm; (*c*) misfit dislocation network with threading dislocation arrowed, $h = 25$ nm.

(d) The surface, including the grid, was covered with melted black wax.
(e) The specimen was immersed in 10% HF for 5–15 h.
(f) The wax was dissolved in trichloroethylene, leaving a grid-mounted TEM specimen.

3.3. Electron microscopy

The TEM specimens were observed in a JEOL 2000FX transmission electron microscope operated at 200 kV. The dislocation density for each specimen was estimated by

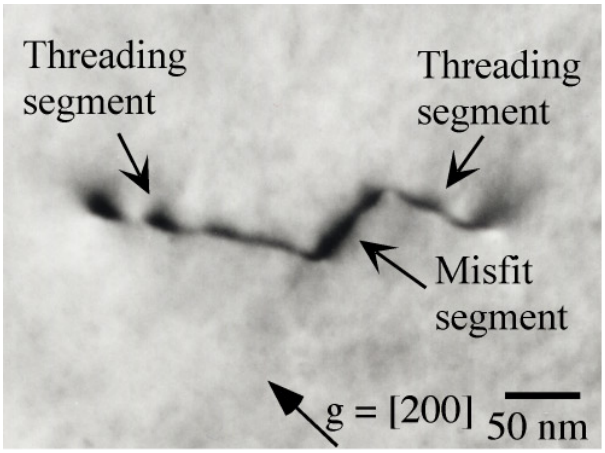

(*a*)

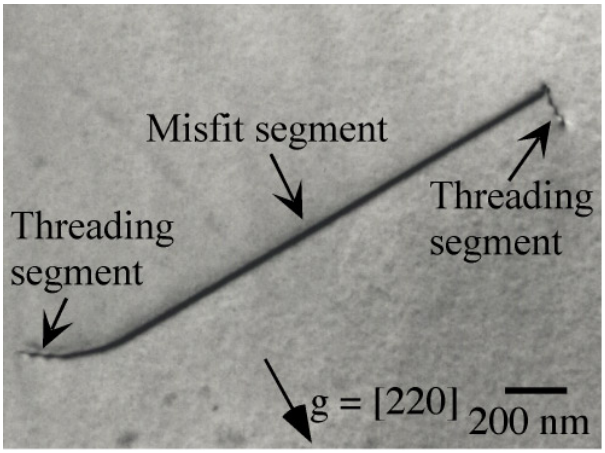

(*b*)

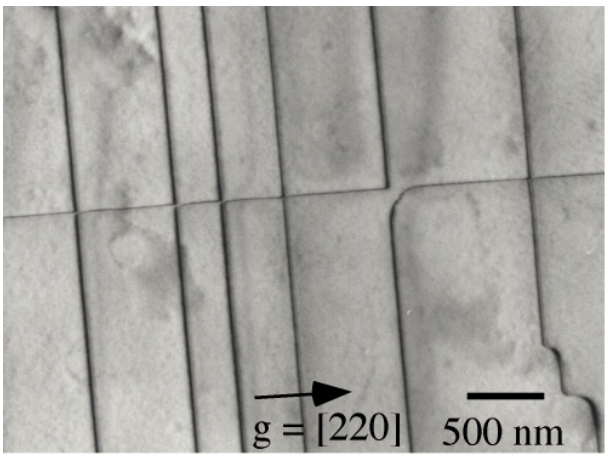

(*c*)

Figure 6. Dislocations in $GaAs/In_{0.2}Ga_{0.8}As/GaAs$: (*a*) misfit dislocation segment, $h = 4$ nm; (*b*) elongated misfit dislocation segment, $h = 10$ nm; (*c*) misfit dislocation network, $h = 20$ nm.

averaging the dislocation line length per unit volume over a series of adjacent regions.

A preliminary check was made to establish whether dislocations could be introduced, or the configuration of existing ones could be changed, during specimen preparation. A selection of specimens was therefore observed before and after ELO using cathodoluminescence (CL) with a JEOL JSM-820 scanning electron microscope. Figure 3 shows the CL images obtained from the same areas of the same specimens before and after ELO. It can been seen that the dislocation configurations were unchanged by the process.

4. TEM observations

The three layer thicknesses for each value of indium concentration, x, fall into the three regions delineated by the critical thickness curves in figure 2. For $x = 0$, i.e. continuous GaAs, the only dislocations observed are threading dislocations with a density of approximately 10^5 cm^{-2} (figure 4).

Figure 5(*a*) shows the geometry of dislocations observed from specimens where $x = 0.15$ and the designed value of h was 6 nm, which is less than either h_c (8.6 nm) or H_c (20.9 nm). Verification of h by cross-sectional TEM yielded a value of 6.4 ± 0.5 nm. Even if x were in fact 5% greater, at the limit of its accuracy, h would still be less than h_c, which would become 8.0 nm.

Figure 5(*a*) shows that the threading dislocations have been divided into two segments by a short dislocation segment. This segment lies in the $[1\bar{1}0]$ direction and its Burger's vector is $(a/2)[0\bar{1}1]$ [2]. It is therefore a 60° misfit dislocation formed by glide on the (111) slip plane. The total dislocation density in these specimens was only marginally higher than in the specimens of continuous GaAs, and so was still approximately 10^5 cm^{-2}. The dislocation geometry in figure 5(*a*) is not an isolated case; most of the threading dislocations have been similarly affected. The formation of these misfit segments in threading dislocations marks the onset of relaxation, i.e. stage II of the model, even though the strained-layer thickness in these specimens is below both h_c and H_c.

At a larger strained-layer thickness (h) of 15 nm, which is above h_c but still below H_c, the misfit dislocation segments were elongated as shown in figure 5(*b*). These elongated misfit segments lie in the interface that was closest to the substrate prior to ELO. The total dislocation density was measured as 4×10^5 cm^{-2} and thus had not risen significantly.

At the largest strained-layer thickness (h) of 25 nm, which is above H_c, a network of misfit dislocations was observed, as shown in figure 5(*c*). Not all threading dislocations have produced misfit segments, however; an example is marked. The total dislocation density had increased substantially to 5×10^8 cm^{-2}.

Figure 6 shows that a similar set of results were observed when $x = 0.2$ and the designed strained-layer thicknesses, h, were 4, 10 and 20 nm. As $h_c = 5.8$ nm and $H_c = 14.5$ nm, these specimens correspond to $h < h_c$, $h_c < h < H_c$, and $h > H_c$ respectively. Verification of h by cross-sectional TEM yielded a value of 4.6 ± 0.5 nm for the thinnest layer. Even if x were in fact 5% greater, at the limit of its accuracy, this thickness is still less than h_c, which would become 5.4 nm.

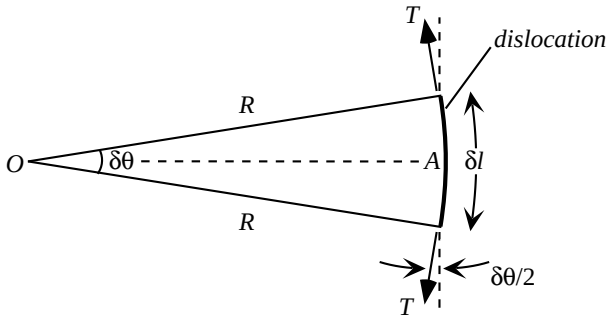

Figure 7. Bowed element of dislocation under line tension forces T.

5. Discussion

The TEM observations have confirmed the mechanism of formation of misfit dislocations from threading dislocations as a means of relieving stress in strained-layer structures, in accordance with the M–B model. While the strained layer was originally being grown by MBE, it was bounded by only one interface. Thus the appropriate value of critical thickness given by the M–B model is h_c rather than the larger value H_c. However, misfit dislocation segments were observed to form at a strained-layer thickness, h_c', slightly smaller even than h_c. This observation was repeatable at numerous locations in a given specimen, and in different specimens.

Previous experimental observations of critical thickness have found values to be higher than predicted by the M–B model [12–14], rather than lower as reported here. For this reason, some authors [14, 15] have proposed temperature-dependent modifications to the M–B model which raise the critical thickness at low growth temperatures. However, the minute changes in dislocation structure shown in figures 5(*a*) and 6(*a*) would not have been observed by techniques which rely on the detection of strain relaxation. Thus the observation reported here of a lower critical thickness necessitates a reappraisal of the M–B model.

While a strained-layer structure is being grown, threading dislocations are 'grown in' across the interfaces. The stress due to misfit strain resolved onto a dislocation line δl crossing the interface is given by

$$\tau_\varepsilon = \frac{2G(1+\nu)}{1-\nu}\varepsilon S$$

where S is an angular factor.

The largest force resisting the formation of a misfit dislocation considered by the model is the line tension. The direction of the net force due to line tension on a bowing dislocation is perpendicular to the dislocation and towards the centre of curvature (figure 7) [16]. The dislocation will only remain curved if there is a shear stress which produces a force on the dislocation line in the opposite direction. The shear stress needed to maintain a radius of curvature is τ_0, and the outward force along OA due to the shear stress acting on the dislocation is $\tau_0 b\,\delta l$. The opposing inward force along OA due to the line tension T is $2T\sin(\delta\theta/2)$ which is equal to $T\delta\theta$ for small values of $\delta\theta$. Thus, the line tension is given by

$$T = \tau_0 b\frac{\delta l}{\delta\theta}.$$

During MBE growth, a single strained layer of $In_xGa_{1-x}As$ is deposited before the next GaAs layer. A short threading dislocation segment δl would be grown into this layer. If the segment were to begin to bow, the component of T along the interface, $T\delta\theta$, would provide a small resistive force against the bowing.

A number of other factors that resist dislocation elongation have been considered [1, 17], which would have the effect of raising the theoretical critical thickness rather than lowering it. When a misfit dislocation segment is produced, a surface step is created. The force resisting the creation of a surface step is

$$F_s = \tau_s b S'$$

where S' is an angular factor and τ_s is the surface tension stress. The latter is assumed to be given by [18]

$$\tau_s = Gb/8$$

and is much smaller than the misfit stress within the range of the misfit concerned here.

Dislocation motion may also be retarded by point defects or solute atoms which segregate to the dislocation [19, 20]. It has been pointed out [17] that, as the threading dislocations are grown in during MBE deposition, it is likely that the dislocation cores will be decorated. The dislocations are thereby pinned so that additional stress is required to overcome the static friction force. As soon as a threading dislocation starts to elongate, it breaks away from the decoration and the static friction force disappears. Because of variable amounts of dislocation decoration, it can be expected that there would be differences in the force required to overcoming pinning for different threading dislocations. This could explain the observation, in figure 5(*c*), of an unchanged threading dislocation among a misfit dislocation network.

When a dislocation starts to move, the lattice resists the motion. The Peierls–Nabarro stress describes the minimum stress required to move a lattice dislocation rigidly and irreversibly. Therefore the shear stress, τ_p, required to make a dislocation glide is [16, 21, 22]

$$\tau_p = \frac{2G}{1-\nu}\exp\left(\frac{-2\pi w}{b}\right)$$

where w is $d/2(1-\nu)$ and d is the interplanar spacing of the crystal. For misfit dislocations in the zincblende lattice, whose Burger's vectors are of the type $(a/2)\langle 110\rangle$, $\tau_\varepsilon \gg \tau_p$ at typical values of ε. Thus the resisting forces on a dislocation line δl in the direction parallel to the interface are outweighed by the force due to the misfit stress. It is therefore proposed that glide of a dislocation segment δl in a {111} plane takes place before it has an opportunity to bow. This would give rise to misfit dislocations in the (001) interface in the same way as the M–B model. However, the critical thickness would be reduced compared with the M–B model, which assumes that the dislocations bow. The TEM observations in figures 5(*a*) and 6(*a*), showing a misfit segment forming in only one of the two interfaces, support the occurrence of glide rather than the bowing shown in figure 1.

If critical thickness is regarded as the point at which the force due to misfit strain exceeds the resistive force due to line

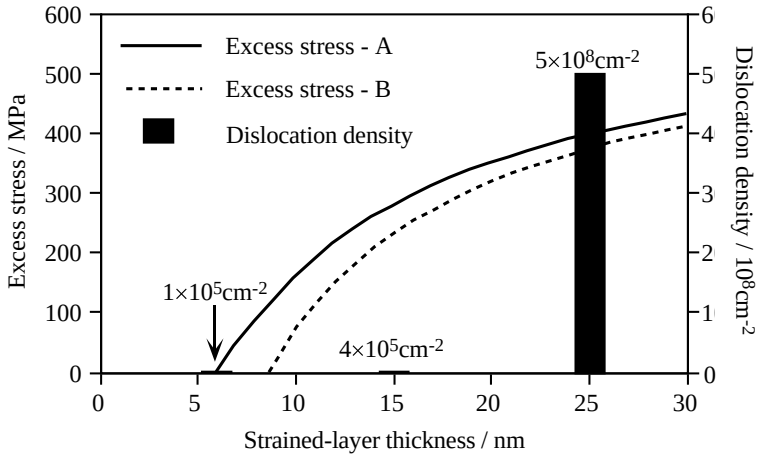

Figure 8. Misfit dislocation density and excess stress versus strained-layer thickness, h, for $GaAs/In_{0.15}Ga_{0.85}As/GaAs$. Curve B is calculated according to the M–B model while curve A is from the same calculation but with the start point shifted to a lower h according to experimental observation.

tension, the misfit dislocations would be expected to extend further as the strained layer thickness increases beyond the critical value. The extension of the misfit dislocations would be expected to be proportional to the excess stress [23], τ_{ex}, given by

$$\tau_{ex} = \tau_\varepsilon - \tau_l$$

where τ_l is the stress due to line tension. Figure 8 shows how τ_{ex} increases with h in $In_{0.15}Ga_{0.85}As/GaAs$ heterostructures. However, the dislocation density does not increase in this manner. In figure 5(*a*), where the formation of misfit dislocations had begun, the total dislocation density is 10^5 cm^{-2}. When the strained layer is more than twice as thick (figure 5(*b*)) and the excess stress is therefore much greater (figure 8), the dislocation density is still only 4×10^5 cm^{-2}. However, when the strained layer thickness reaches approximately $4h_c'$ (figure 5(*c*)), the dislocation density suddenly increases to 5×10^8 cm^{-2} and the structure is relaxed. This observed sudden change in dislocation density, also shown in figure 8, suggests that only local relaxation is caused by a mechanism based on the formation of misfit dislocation segments from existing threading dislocations. A different mechanism dominates the global relaxation process.

6. Conclusions

Four different geometries of dislocation can be classified for the different $GaAs/In_xGa_{1-x}As/GaAs$ structures:

(a) straight threading dislocations in GaAs;
(b) threading dislocations with misfit segments when the strained-layer thicknesses h are slightly below the critical thickness h_c predicted by the M–B model;
(c) elongated misfit dislocations when $h_c < h < H_c$;
(d) misfit dislocation network when $h > H_c$.

It is proposed that the initial stage of misfit dislocation formation occurs by glide of threading dislocations at the interfaces in $GaAs/In_xGa_{1-x}As/GaAs$ double heterostructures. This process can take place at strained-layer thicknesses below the critical value predicted by the M–B mechanism and is thus consistent with the experimental observations reported here. As the strained-layer thickness is increased beyond its critical value for a single heterostructure, h_c, the dislocation density does not alter significantly until a sudden change occurs above the double-heterostructure critical thickness, H_c. This suggests that the formation of misfit dislocations from threading dislocations, which is the basis of the M–B model, is not the main relaxation mechanism.

Acknowledgments

Financial support from the Open University Research Committee is acknowledged. The authors are grateful to N Williams for technical support and to P Augustus of GEC Materials Technology Ltd for the cross-sectional TEM thickness measurements.

References

[1] Matthews J W, Mader S and Light T B 1970 *J. Appl. Phys.* **41** 3800
[2] Matthews J W and Blakeslee A E 1974 *J. Cryst. Growth* **27** 118
[3] Matthews J W 1975 *J. Vac. Sci. Technol.* **12** 126
[4] Pichaud B, Putero M and Burle N 1999 *Phys. Status Solidi* A **171** 251
[5] Hull R and Stach E A 1996 *Curr. Opinion Solid State Mater. Sci.* **1** 21
[6] Downes J R, Dunstan D J and Faux D A 1997 *Philos. Mag.* **76** 77
[7] Dunstan D J 1997 *J. Mater. Sci.: Mater. Electron.* **8** 337
[8] Dixon R H and Goodhew P J 1990 *J. Appl. Phys.* **68** 3163
[9] Whitehouse C R, Barnett S J, Usher B F, Cullis A G, Keir A M, Johnson A D, Clark G F, Tanner B K, Spirkl W, Lunn B, Hagston W and Hogg C 1993 *Microscopy of Semiconducting Materials 1993 (Inst. Phys. Conf. Ser. 134)* ed Cullis *et al* (Bristol: Institute of Physics Publishing) p 563
[10] Kidd P, Fewster P F, Andrew N L and Dunstan D J 1993 *Microscopy of Semiconducting Materials 1993 (Inst. Phys. Conf. Ser. 134)* ed Cullis *et al* (Bristol: Institute of Physics Publishing) p 585
[11] Rhan H 1996 *Properties of III–V Quantum Wells and Superlattices* (Short Run Press)

[12] Whaley G J and Cohen P I 1990 *Mater. Res. Soc. Symp. Proc.* **160** 35
[13] Radulescu D C 1989 *J. Vac. Sci. Technol.* B **7** 111
[14] Price G L 1991 *Phys. Rev. Lett.* **66** 469
[15] Fox B A and Jesser W A 1990 *J. Appl. Phys.* **68** 2801
[16] Hull D and Bacon D J 1992 *Introduction to Dislocations* 3rd edn (Oxford: Pergamon)
[17] Zuo J, Cockayne D J H and Usher B F 1993 *J. Appl. Phys.* **73** 619
[18] Matthews J W, Blakeslee A E and Mader S 1976 *Thin Solid Films* **33** 253
[19] Jesser B A and Jesser W A 1990 *J. Appl. Phys.* **68** 2801
[20] Jesser W A and Fox B A 1990 *J. Electron. Mater.* **19** 1289
[21] Kovacs I and Zsoldos L 1973 *Dislocations and Plastic Deformation* (Oxford: Pergamon)
[22] Wang J N 1996 *Acta Mater.* **44** 1541
[23] Dodson B W and Tsao J Y 1987 *Appl. Phys. Lett.* **51** 1325